International Journal of Bifurcation and Chaos, Vol. 20, No. 5 (2010) 1499–1507

DOI: 10.1142/S0218127410026642

PERIODICALLY FORCED CHAOTIC SYSTEM WITH SIGNUM NONLINEARITY

KEHUI SUN[*,†,‡] and J. C. SPROTT[†,§]
[*]*School of Physics Science and Technology,*
Central South University, Changsha 410083, China
[†]*Department of Physics,*
University of Wisconsin Madison, WI 53706, USA
[‡]*kehui@csu.edu.cn*
[§]*sprott@physics.wisc.edu*

Received July 10, 2009; Revised August 3, 2009

A sinusoidally-driven system with a simple signum nonlinearity term is investigated through an analytical analysis as well as dynamic simulation. To obtain the correct Lyapunov exponents, the signum function is replaced by a sharply varying continuous hyperbolic tangent function. By phase portraits, Poincaré sections and bifurcation diagrams, the rich dynamic behaviors of this system are demonstrated, such as an onion-like strange attractor, pitchfork and attractor merging bifurcations, period-doubling routes to chaos, and chaotic transients in the case of small damping. Moreover, the chaos persists as the damping is reduced to zero.

Keywords: Chaos; nonautonomous systems; differential equations; bifurcations; signum function.

1. Introduction

It has been known that many nonlinear functions can generate chaos. Some of the earliest examples of chaos occur in periodically forced nonlinear oscillators, which have the form $\ddot{x} + f(\dot{x}, x) = F \sin \omega t$, where the function $f(\dot{x}, x)$, contains at least one nonlinearity in the damping ($\dot{x}$) term or the restoring force (x) term. For example, the van der Pol equation has an x^2 in the damping term [van der Pol, 1926], while the Rayleigh differential equation [Birkhoff & Rota, 1978] is similar to the van der Pol equation but has an $\dot{x}^2$ nonlinearity in the damping. More common and more widely studied is the system in which the damping is linear, but the restoring force contains a cubic nonlinearity, such as the Duffing oscillator [Duffing, 1918], the Ueda oscillator [Ueda, 1979], Duffing's two-well oscillator [Moon & Holmes, 1979], as well as a variant of this function [Bonatto *et al.*, 2008] without the linear term in x. Several hybrid chaotic forced oscillators have been studied by combining two cases such as the Rayleigh–Duffing oscillator [Hayashi *et al.*, 1970] and the Duffing–van der Pol oscillator [Ueda, 1992]. Additionally, quadratic functions in the restoring force term can also suffice to give chaos in a forced oscillator [Tang *et al.*, 2001]. Other systems in which $f(\dot{x}, x)$ is a more complicated nonlinear function have been studied [Scheffczyk *et al.*, 1991]. A simpler nonlinearity is a piecewise linear function involving a single absolute value. Piecewise linear oscillators with more than two linear regions that produce chaos when periodically forced have been extensively studied, for example, using Chua's diode [Murali *et al.*, 1994; Srinivasan, 2008], and using damping control for a chaotic impact oscillator [Souza *et al.*, 2007]. Whereas the absolute value is a continuous piecewise-linear function, discontinuous functions sometimes arise in models of real applications. An example is a harmonic oscillator

with Coulomb damping [Feeny, 1992]. For a forced oscillator, the simplest such case would be $f(\dot{x}, x) = \dot{x} - x + \mathrm{sgn}(x)$, which is arguably simpler than the so-called "simplest sinusoidally-forced chaotic system" studied in [Gottlieb & Sprott, 2001] which involves an x^3 nonlinearity. Here, we are interested in the case where the only nonlinearity is the signum function in the restoring force term. It is well known that the signum function describes a class of simple discontinuous switching structures, or one type of the most important nonsmooth structures. On one hand, a simple nonsmooth structure may easily create complex phenomena, and therefore, nonsmooth technique has gradually become a powerful strategy for generating complex dynamics in simple autonomous systems [Chen *et al.*, 2006]. On the other hand, switching schemes usually can be simply structured and easily designed with cost-effective electronic circuit realizations.

The plan of the paper is as follows. In Sec. 2, we present the forced oscillator and its attractor. In Sec. 3, the system equations are briefly investigated through analytical solutions in the respective linear regions. In Sec. 4, we describe the dynamics and bifurcations of the forced system. Finally, we summarize the results and indicate future directions.

2. The Periodically Forced Oscillator

Consider the following nonautonomous differential equation

$$\ddot{x} + a\dot{x} - x + b\,\mathrm{sgn}(x) = F\sin(\omega t), \tag{1}$$

where, a, b, F, ω are positive constants, and $\mathrm{sgn}(x)$ is the signum function which is either $+1$ or -1 depending on whether its argument x is positive or negative, respectively. This system resembles the Duffing oscillator except that the nonlinearity is in the low order term rather than in the high order term. For simplicity, we shall set the parameter $\omega = 1$ as described in [Thompson, 1997], and regard a, b, and F as the control parameters. The "onion-like" strange attractor is observed by choosing appropriate parameters as shown in Fig. 1 with the largest Lyapunov exponent of 0.1241, and the Kaplan–Yorke dimension $D_{\mathrm{KY}} = 2.134$.

It is instructive to examine the solution of Eq. (1) in phase space. For this purpose, rewrite Eq. (1) with $\omega = 1$ in terms of x and y as

$$\begin{cases} \dot{x} = y, \\ \dot{y} = -ay + x - b\,\mathrm{sgn}(x) + F\sin(t). \end{cases} \tag{2}$$

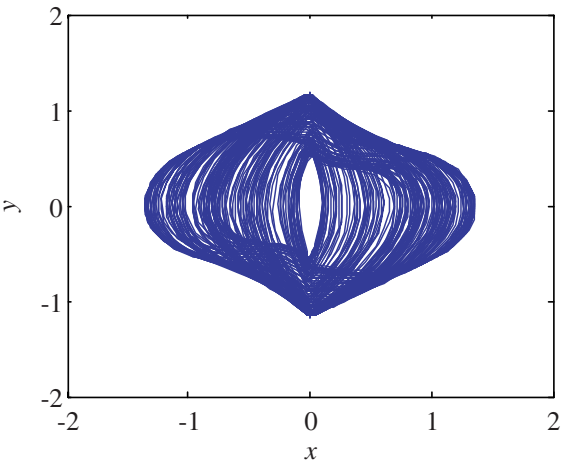

Fig. 1. The onion-like attractor of Eq. (1) with $a = 1.05$, $b = 1, F = 1.1$, and $\omega = 1$.

If we let $z = t$, then the nonautonomous system is converted into an autonomous one, and the two-dimensional system becomes three-dimensional

$$\begin{cases} \dot{x} = y \\ \dot{y} = -ay + x - b\,\mathrm{sgn}(x) + F\sin(z)\,. \\ \dot{z} = 1 \end{cases} \tag{3}$$

3. Analytical Study

3.1. *Explicit analytical solution*

Let us briefly investigate this system equation by an analytical solution in each of the two linear regions. Let D_1 be the subspace where x is positive and D_2 be the subspace where x is negative. D_1 and D_2 are represented as

$$\begin{aligned} D_1 &= \{(t, x_1, \dot{x}_1) \mid x > 0\}, \\ D_2 &= \{(t, x_2, \dot{x}_2) \mid x < 0\}. \end{aligned} \tag{4}$$

In each of the regions D_1 and D_2, Eq. (1) is linear when $F = 0$. The stability depends on the eigenvalues of the equation $\lambda^2 + a\lambda - 1 = 0$, which are found to be $(-a \pm \sqrt{a^2 + 4})/2$. Consequently the equilibrium points in both the D_1 and D_2 regions are saddle points, either $a > 0$ or $a < 0$. Then Eq. (1) can be represented as a single second-order inhomogeneous linear differential equation in each of the regions D_1 and D_2 as

$$\ddot{x} + a\dot{x} - x = F\sin(\omega t) - b \quad x > 0, \tag{5a}$$

and

$$\ddot{x} + a\dot{x} - x = F\sin(\omega t) + b \quad x < 0. \tag{5b}$$

Equation (2) can be explicitly integrated in terms of elementary functions in each of the regions D_1 and

D_2 and matched across the boundaries to obtain the full solution as shown below.

The general solution to Eq. (5a) can be easily written as

$$x(t) = Ae^{\lambda_1 t} + Be^{\lambda_2 t} + E_1 \sin \omega t + E_2 \cos \omega t - b, \quad (6)$$

where A and B are constants of integration and

$$E_1 = \frac{F(1+\omega^2)}{[a^2\omega^2 - (1+\omega^2)^2]} \quad (7)$$

$$E_2 = \frac{Fa\omega}{[a^2\omega^2 - (1+\omega^2)^2]}. \quad (8)$$

Then $\dot{x}(t)$ is obtained from Eq. (6) as

$$\dot{x}(t) = A\lambda_1 e^{\lambda_1 t} + B\lambda_2 e^{\lambda_2 t} + E_1\omega \cos \omega t - E_2\omega \sin \omega t. \quad (9)$$

From Eq. (2), it follows that

$$y = \dot{x}(t). \quad (10)$$

The constants A and B in the above equations can be evaluated by solving both Eqs. (6) and (9) at a suitable initial state with x_0 and y_0 as initial conditions at time $t = t_0$. The constants A and B can be obtained from Eqs. (6) and (9) as

$$A = \frac{e^{-\lambda_1 t_0}}{\lambda_2 - \lambda_1}[x_0 - \lambda_2 y_0 + (E_2\lambda_2 - E_1\omega)\cos \omega t_0 + (E_2\omega + E_1\lambda_2)\sin \omega t_0 \mp b\lambda_2], \quad (11)$$

$$B = \frac{e^{-\lambda_2 t_0}}{\lambda_2 - \lambda_1}[x_0 - \lambda_1 y_0 + (E_2\lambda_1 - E_1\omega)\cos \omega t_0 + (E_2\omega + E_1\lambda_1)\sin \omega t_0 \mp b\lambda_1], \quad (12)$$

where $\mp$ represent D_1 and D_2 regions respectively.

3.2. *The associated Hamiltonian function*

Using the kinetic energy function $y^2/2$ and the potential energy function $-x^2/2 + b|x|$ for system (2), we can define the system Hamiltonian function as

$$H(x, y) = \frac{1}{2}y^2 - \frac{1}{2}x^2 + b|x|. \quad (13)$$

This function is piecewise defined, and is continuous but not differentiable at (and only at) $x = 0$. On the level set $H(x, y) = 0$ with $y = 0$, it has three zeros: $x_0 = 0$ and $x_{1,2} = \pm 2b$ as shown in Fig. 2. It shows that system (1) is similar to the Duffing system for the case with the restoring force of the form $x - 0.4x^3$ [Sprott, 2003].

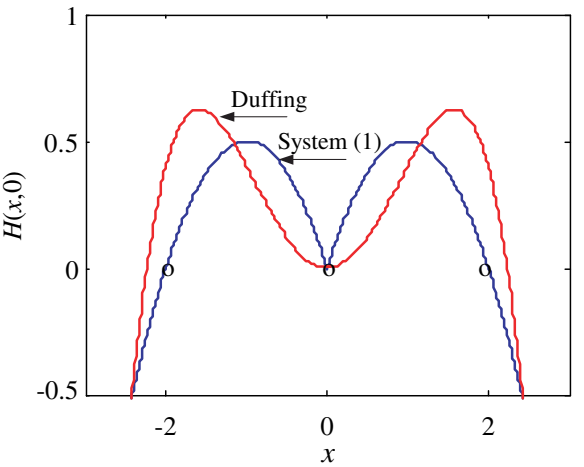

Fig. 2. The Hamiltonian function of system (1) and Duffing oscillator with one potential well.

4. Dynamical Behaviors

4.1. *Calculating the largest Lyapunov exponent*

Lyapunov exponents are the best indicators to categorize the different classes of nonlinear phenomena. A positive Lyapunov exponent confirms chaos. If the system equations are known, algorithms [Parker & Chua, 1989] can readily be applied to compute the largest or all of the exponents. Alternatively, the method of embedded dimensions may be applied to a time series resulting from simulations and experiments to estimate their exponents [Wolf *et al.*, 1985]. But these approaches do not work satisfactorily for nonsmooth systems, i.e. those where the vector field is not continuously differentiable. For example, if parameters $a = 1.4$, $b = 1$, $F = 1.1$, $\omega = 1$, and initial condition [0.7065, −0.1282, 500] in Eq. (1), then the system is a limit cycle as shown in Fig. 3(a). But the calculated largest Lyapunov exponent is 0.5204, which is evidently incorrect, and is an example of the chaotic limit cycle paradox as described in [Grantham & Lee, 1993]. To calculate the largest Lyapunov exponent of system (1) correctly, the signum function can be replaced by continuous equivalents [Gans, 1995],

$$\text{sgn}(x) \to \tanh(nx),$$

where n is a large constant. The question is how to determine a suitable value for n. We calculate the largest Lyapunov exponent versus n for states of limit cycle [Fig. 3(a)] and chaos [Fig. 3(c)] in system (1) respectively, and the curves are presented in Figs. 3(b) and 3(d). As shown in Figs. 3(b) and 3(d), if n is a very small number, then the hyperbolic

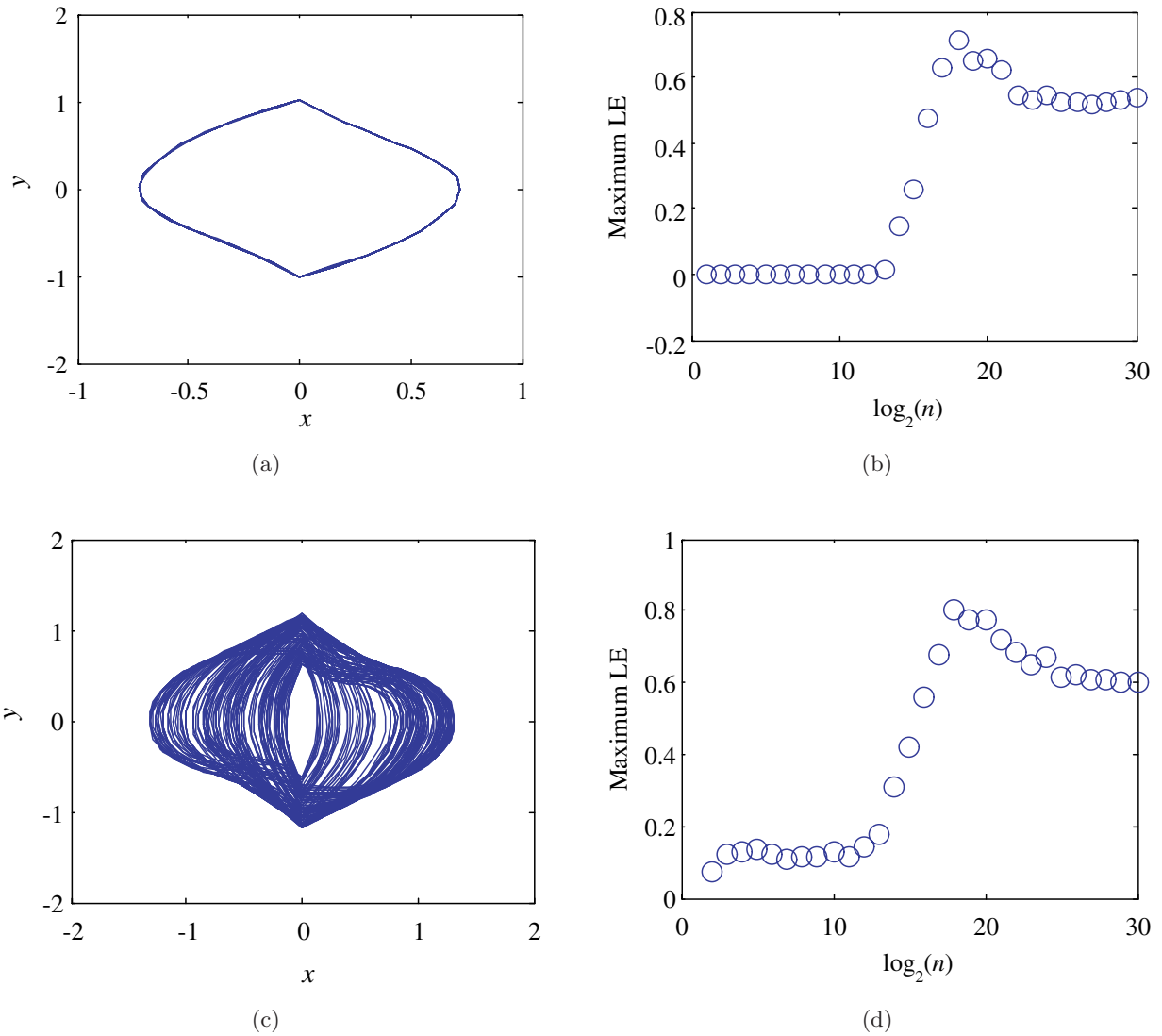

Fig. 3. Phase portraits and their maximum Lyapunov exponent versus n. (a) Limit cycle. (b) Maximum Lyapunov exponent for limit cycle. (c) Chaos. (d) Maximum Lyapunov exponent for chaos.

tangent is far from the signum function. If n is a much larger number, the hyperbolic tangent is nearly equal to the signum function. The results are unreliable in these limits. So, for system (1), n can be chosen from 2^3 to 2^{12}, in which range the calculated Lyapunov exponent is independent of n. After the signum function is replaced by tanh with $n = 1000$, the largest Lyapunov exponent of the limit cycle shown in Fig. 3(a) becomes -3.6885×10^{-4}.

4.2. *Bifurcations and route to chaos*

To study the dynamics of system (1), three cases were considered as follows.

(1) Fix $b = 1$ and $F = 1.1$, and vary a. The system is calculated numerically with $a \in [1, 1.45]$ for an increment of $\Delta a = 0.0005$. The bifurcation diagram is shown in Fig. 4(a). A pitchfork bifurcation occurs at $a = 1.365$, and two attractors, denoted in blue and red, respectively, coexist when the parameter is less than 1.365. An attractor-merging crisis bifurcation occurs in this case. The attractors grow larger as a decreases, until they collide at $a = 1.07$. Thus two separate attractors merge into one and remain bounded until $a = 1.04$. If the orbit is initially confined to one of the attractors, the region occupied by it suddenly doubles in size at the crisis point. With an increase in the value of the parameter a, a reverse period-doubling phenomenon is observed. The largest Lyapunov exponent of the system (1) was computed numerically for $a \in [1.05, 1.4]$ in increments of $\Delta a = 0.01$ and is shown in Fig. 4(d). It is evident that chaos exists for $1.05 \leq a \leq 1.1$.

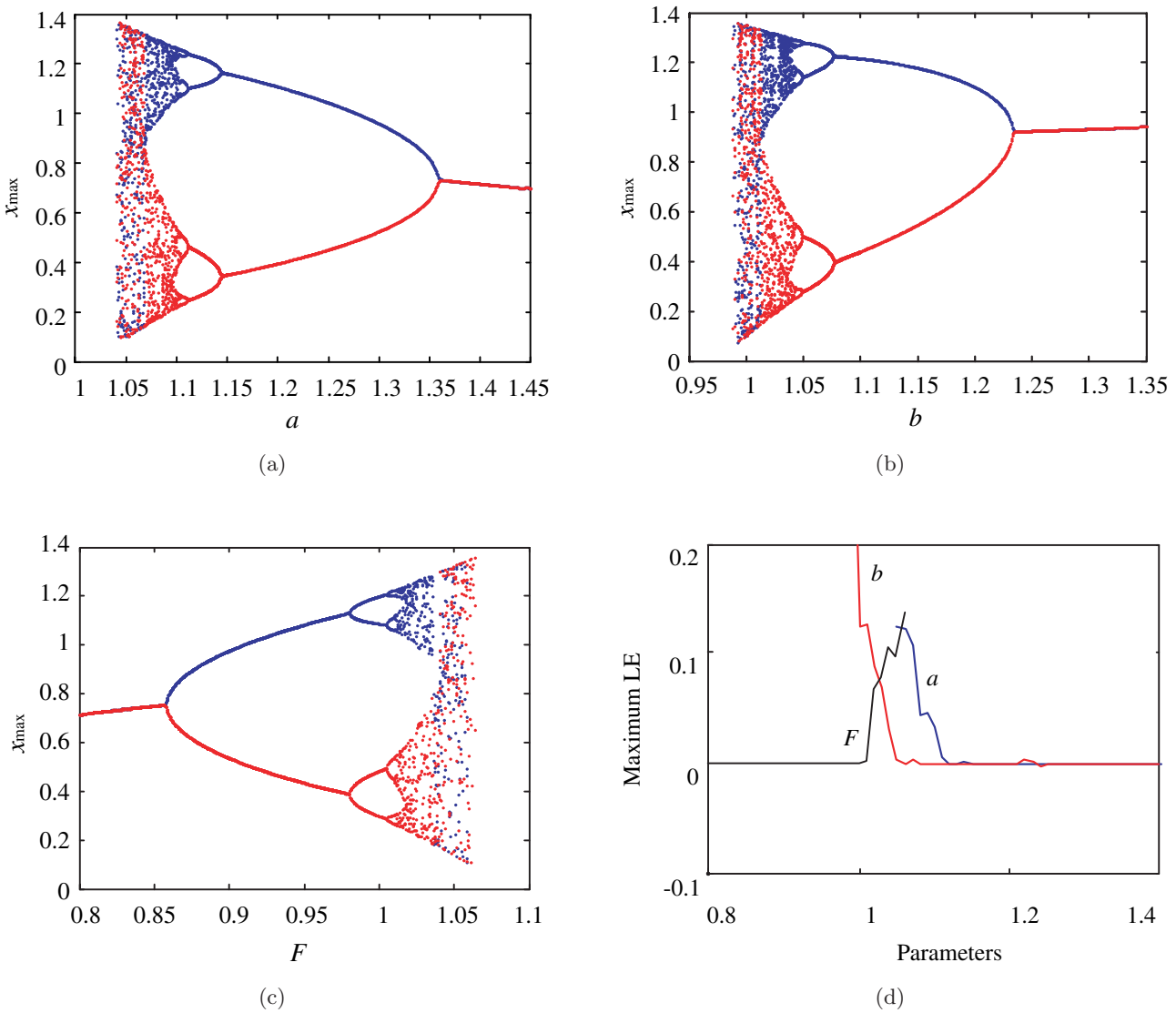

Fig. 4. Bifurcation and largest LE diagrams with different control parameters for Eq. (1). (a) $b = 1$, $F = 1.1$. (b) $a = 1.05$, $F = 1.1$. (c) $a = 1$, $b = 1$. (d) Diagram of largest LE.

(2) Fix $a = 1.05$ and $F = 1.1$, and vary b. The system is calculated numerically with $b \in [0.95, 1.35]$ for an increment of $\Delta b = 0.0005$. The bifurcation diagram is shown in Fig. 4(b). A pitchfork bifurcation occurs at $b = 1.24$, and two attractors, denoted in blue and red, respectively, coexist when the parameter is less than 1.24. An attractor-merging crisis bifurcation occurs in this case. The attractors grow larger as b decreases, until they collide at $b = 1.03$. Thus two separate attractors merge into one and remain bounded until $b = 0.99$. If the orbit is initially confined to one of the attractors, the region occupied by it suddenly doubles in size at the crisis point. For an increase in the value of the parameter b, a reverse period-doubling phenomenon is also observed. The largest Lyapunov exponent of the system (1) was computed numerically for $b \in [1, 1.4]$ in increments of $\Delta b = 0.01$ and is shown in Fig. 4(d). It is evident that chaos exists for $1 \leq b \leq 1.05$.

(3) Fix $a = 1$ and $b = 1$, and vary F. The system is calculated numerically with $F \in [0.8, 1.1]$ for an increment of $\Delta F = 0.0005$. The bifurcation diagram is shown in Fig. 4(c). A pitchfork bifurcation occurs at about $F = 0.855$, and two attractors, denoted in blue and red, respectively, coexist when the parameter is larger than 0.855. An attractor-merging crisis bifurcation occurs in this case. The attractors grow larger as F increases, until they collide at $F = 1.04$. Thus two separate attractors merge into one and remain bounded until $F = 1.06$. If the orbit is

initially confined to one of the attractors, the region occupied by it suddenly doubles in size at the crisis point. With an increase in the value of parameter F, a period-doubling phenomenon is observed. The largest Lyapunov exponent of the system (1) was computed numerically for $F \in [0.8, 1.06]$ in increments of $\Delta F = 0.01$ and is shown in Fig. 4(d). It is evident that chaos exists for $1.015 \leq F \leq 1.062$.

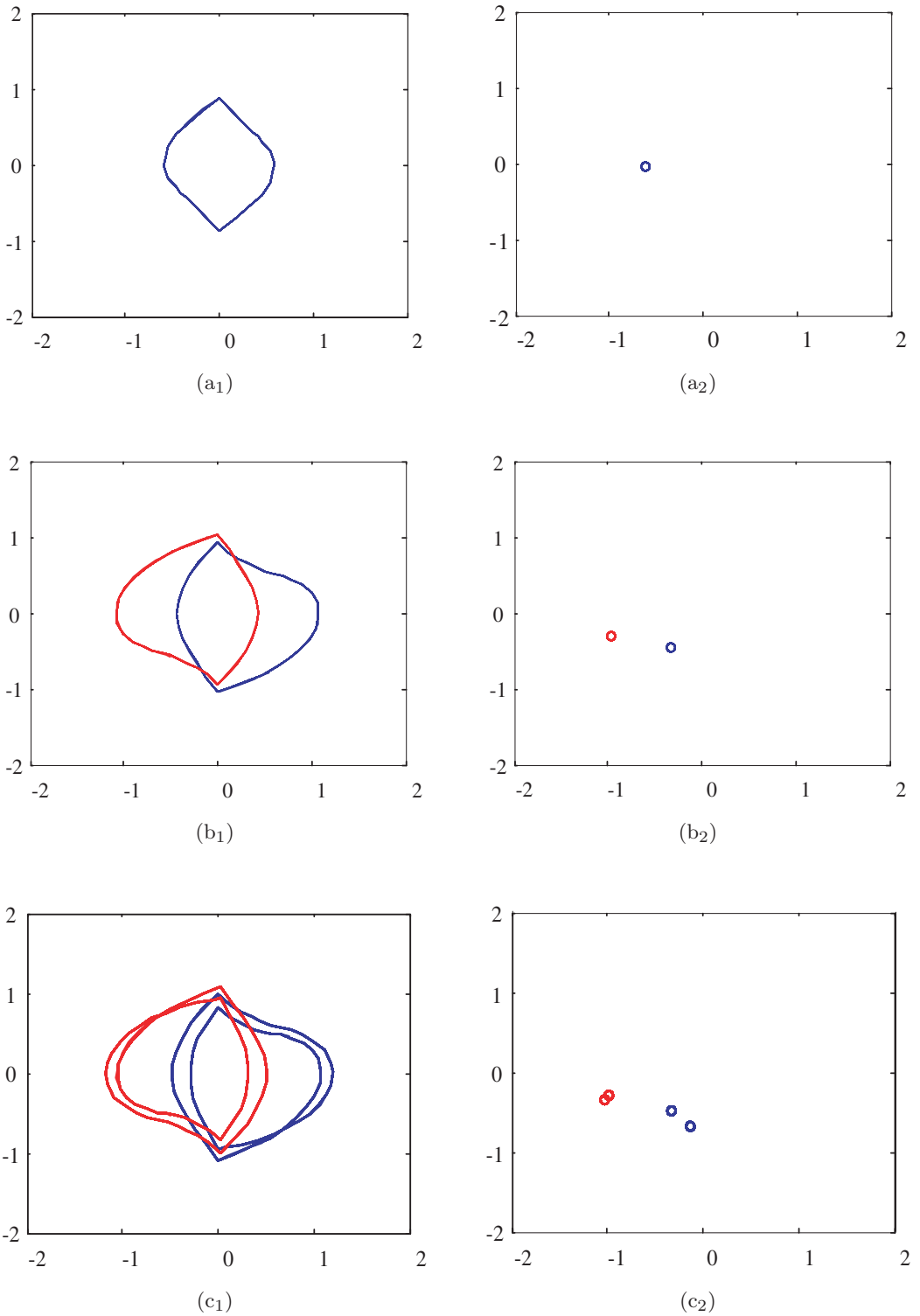

Fig. 5. Phase portraits (left) and Poincaré sections (right) of Eq. (1). (a) $F = 0.65$, one $1T$-periodic solution. (b) $F = 0.95$, two $1T$-periodic solutions. (c) $F = 1$, two $2T$-periodic solutions. (d) $F = 1.01$, two $4T$-periodic solutions. (e) $F = 1.045$, chaotic solution.

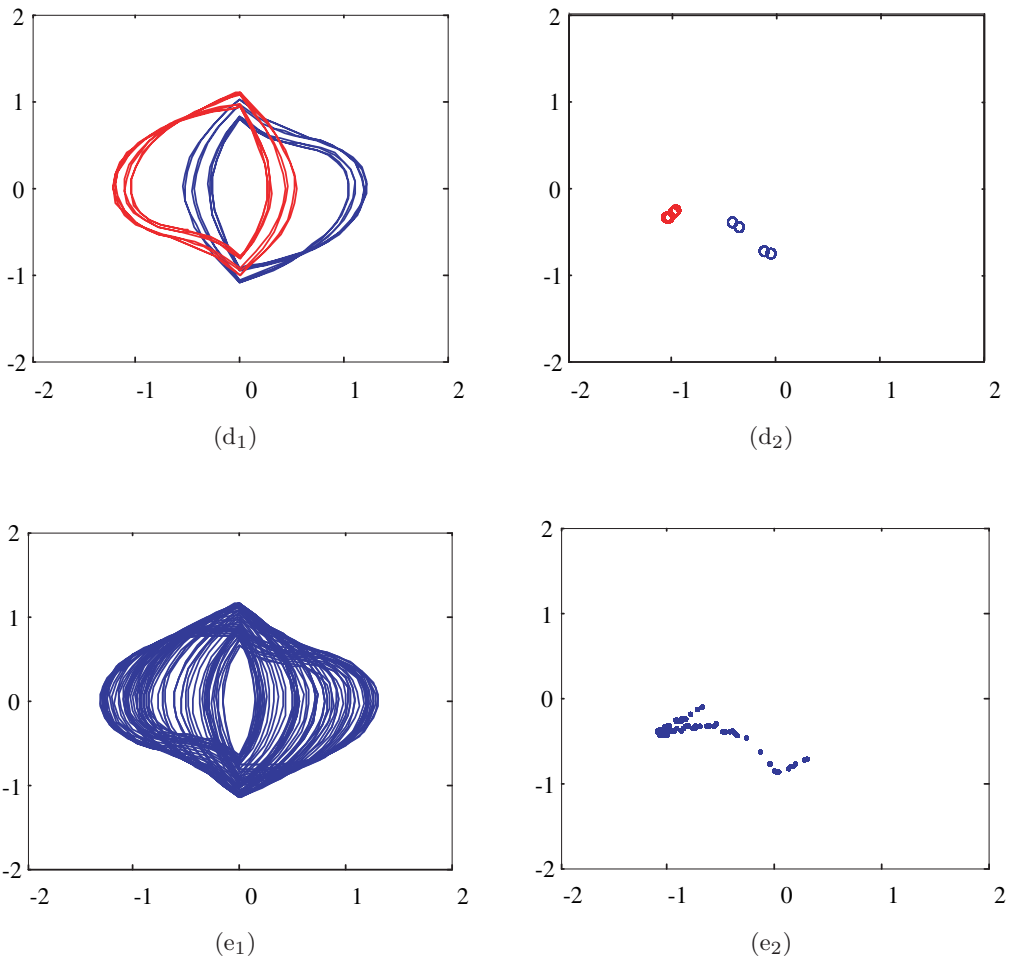

Fig. 5. (*Continued*)

From the three cases above, it can be concluded that selection of appropriate values for the system control parameters can be used to suppress or generate chaos, and that the route to chaos is the same for each of the three parameters.

To observe the route to chaos, the phase portraits and Poincaré sections are presented in Figs. 5(a)–5(e) by fixing $a = b = 1$ but changing the control parameter F. The Poincaré section is in the plane of $z \bmod 2\pi = 1$. Increasing the parameter F, we first observe one limit cycle in the phase portrait as seen in Figs. $5(a_1)$, $5(b_1)$ and one point in the Poincaré sections in Figs. $5(a_2)$, $5(b_2)$, then two cycles as shown in Fig. $5(c_1)$ and two points in Fig. $5(c_2)$, four cycles in Fig. $5(d_1)$, four points in Fig. $5(d_2)$, and finally an infinite number of cycles as shown in Figs. $5(e_1)$ and $5(e_2)$. The route to chaos is by period-doubling bifurcations.

At the same time, when parameter F increases from 0.65 to 1.045, a pitchfork bifurcation and a pair of attractors are born as shown in Fig. 5(b), and then the two coexisting attractors expand as shown in Figs. 5(c) and 5(d) and finally merge by an attractor-merging crisis bifurcation at the onset of chaos as shown in Fig. 5(e).

4.3. *Chaotic transients with small damping*

A phenomenon very common in dynamical systems is that they seem chaotic during some transient period, but finally fall onto a periodic attractor. This phenomenon is said to be a chaotic transient, which has been reported for the standard Lorenz system [Yorke & Yorke, 1979]. Superlong chaotic transients (referred to as "supertransients") have been observed in nonlinear circuit experiments [Zhu *et al.*, 2001]. In such a case, trajectories starting from random initial conditions wander chaotically for an arbitrarily long time before settling into a final attractor that is usually nonchaotic, and the average transient lifetime, which is a function of

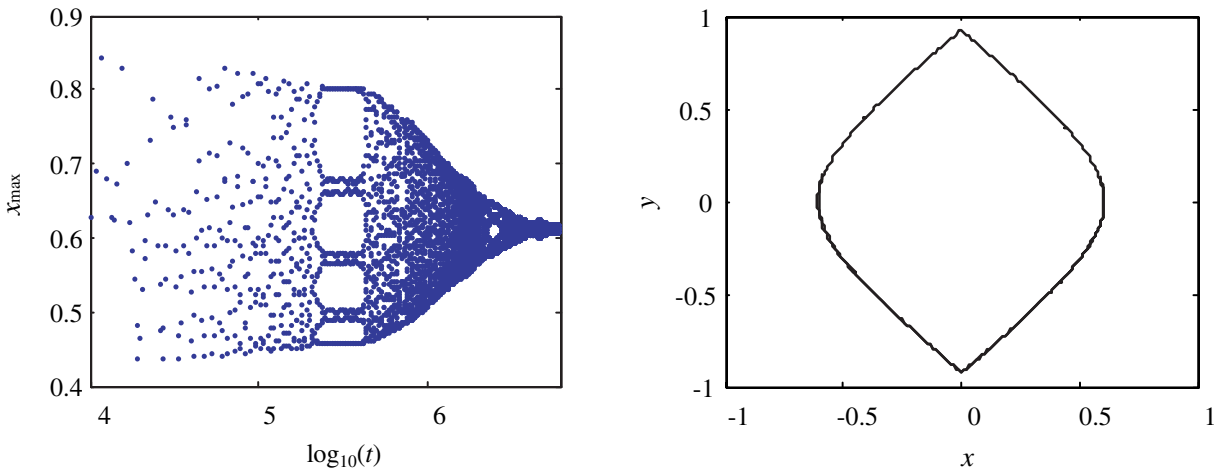

(a) (b)

Fig. 6. Bifurcation diagram and final attractor for Eq. (1) with $a = 0.00015$, $b = 1$ and $F = 0.02$. (a) Chaotic transient. (b) The final attractor.

the damping parameter and external driving force, was studied in [Shen *et al.*, 1997]. Such a situation also occurs in system (1). Choosing initial conditions $[x_0, y_0, z_0] = [0.4589, 0.4262, 0]$ and a small damping parameter $a = 0.00015$, the chaotic transient is shown in Fig. 6(a). It is evident that the trajectory is chaotic with many periodic windows until $t > 6 \times 10^6$, whereupon it finally becomes a limit cycle as shown in Fig. 6(b), and thereafter remains so. It is observed that the transient lifetime is a function of parameters a and F, and when $a \to 0$, the chaotic transient has an infinite lifetime.

4.4. *The undamped oscillator*

If we allow the damping to be zero ($a = 0$) in Eq. (1), then two conservative systems are given by

$$\ddot{x} - x + b\,\mathrm{sgn}(x) = F \sin \omega t, \tag{14}$$

$$\ddot{x} + b\,\mathrm{sgn}(x) = F \sin \omega t. \tag{15}$$

Equation (15) with $f(x) = \mathrm{sgn}(x)$ is especially interesting because it is arguably simpler than the so-called "simplest sinusoidally-forced chaotic system" [Gottlieb & Sprott, 2001] which has a cubic nonlinearity. In fact, it is the special case of the simplest one with $p = 0$ in [Gottlieb & Sprott, 2001]. A trajectory of the conservative system (15) is shown in Fig. 7(a) for initial conditions $[x_0, y_0, z_0] = [1, 0.1, 0]$ and parameters $b = F = \omega = 1$. The largest Lyapunov exponent is 0.0465 in this case. A Poincaré section in the xy-plane for $t \bmod 2\pi = 0.5\pi$ for various initial values of x in the range

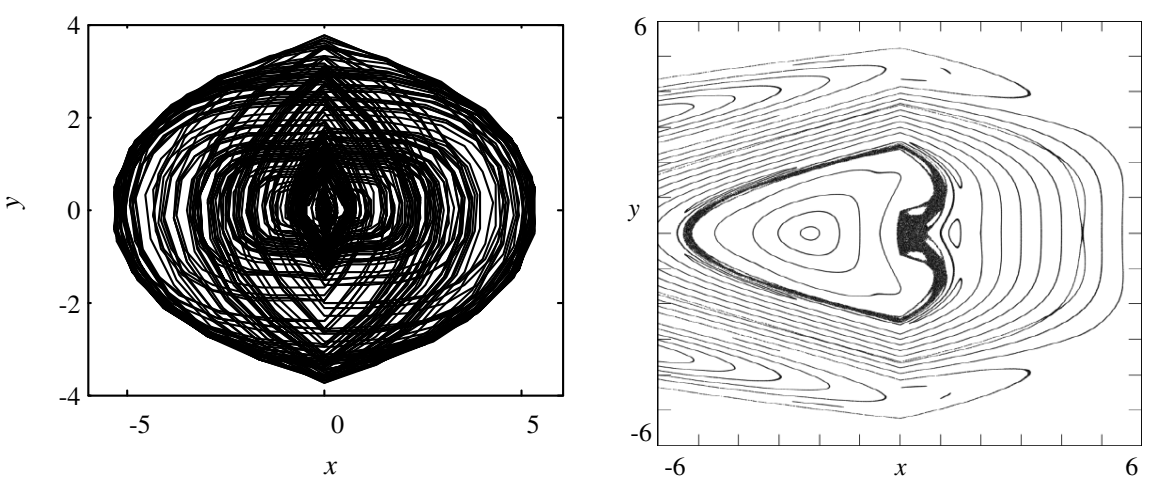

(a) (b)

Fig. 7. Trajectory (a) and Poincaré section (b) of the conservative system in Eq. (15).

$-2 < x_0 < 9$ and $y_0 = 0$, $z_0 = 0.5\pi$ is shown in Fig. 7(b). The chaotic sea is small, as is typical for such periodically forced systems [Sprott, 2003].

5. Conclusions

This paper has reported and analyzed a simple periodically-forced system with a nonlinear function $\mathrm{sgn}(x)$, which can generate chaos for appropriate parameters. The dynamical properties of this chaotic system have been analyzed, including the Lyapunov exponents, bifurcations, routes to chaos and chaotic transients. The results show it has abundant dynamic behaviors. Therefore, research on dynamics of nonlinear systems with a signum nonlinearity has great theoretical significance and practical applications (such as liquid mixing and secure communications). It is worthwhile to explore further simple systems with the signum function to create chaos for different demands.

Acknowledgments

This work was supported by the China Scholarship Council (No. 2006A39010), the National Nature Science Foundation of People's Republic of China (Grant No. 60672041), and the National Science Foundation for Post-doctoral Scientists of People's Republic of China (Grant No. 20070420774). We are grateful for discussions with Prof. George Rowlands.

References

Birkhoff, G. & Rota, G. [1978] *Ordinary Differential Equations*, 3rd edition (John Wiley and Sons: NY).

Bonatto, C., Gallas, J. A. C. & Ueda, Y. [2008] "Chaotic phase similarities and recurrences in a damped-driven Duffing oscillator," *Phys. Rev. E* **77**, 026217-1–026217-5.

Chen, Q. F., Hong, Y. G. & Chen, G. R. [2006] "Chaotic behaviors and toroidal/spherical attractors generated by discontinuous dynamics," *Physica A* **371**, 293–302.

Duffing, G. [1918] *Erzwungene Schwingungen Bei Veranderlicher Eigenfrequenz* (Vieweg: Braunschweig).

Feeny, H. [1992] "A nonsmooth coulomb friction oscillator," *Physica D* **59**, 25–38.

Gans, R. F. [1995] "When is cutting chaotic?" *J. Sound Vibr.* **188**, 75–83.

Gottlieb, H. P. W. & Sprott, J. C. [2001] "Simplest driven conservative chaotic oscillator," *Phys. Lett. A* **291**, 385–388.

Grantham, W. J. & Lee, B. [1993] "A chaotic limit cycle paradox," *Dyn. Contr.* **3**, 159–173.

Hayashi, C., Ueda, Y., Akamatsu, N. & Itakura, H. [1970] "On the behavior of self-oscillatory systems with external force," *Trans. Instit. Electron. Commun. Engin. Japan* **53-A**, 150–158.

Moon, F. C. & Holmes, P. J. [1979] "A magetoelastic strange attractor," *J. Sound Vibr.* **65**, 275–296.

Murali, K., Lakshmanan, M. & Chua, L. O. [1994] "Bifurcation and chaos in the simplest dissipative nonautonomous circuit," *Int. J. Bifurcation and Chaos* **4**, 1511–1524.

Parker, T. S. & Chua, L. O. [1989] *Numerical Algorithms for Chaotic Systems* (Springer-Verlag).

Scheffczyk, C., Parlitz, U., Kurz, T., Knop, W. & Lauterborn, W. [1991] "Comparison of bifurcation structures of driven dissipative nonlinear oscillators," *Phys. Rev. A* **43**, 6495–6502.

Shen, J., Yin, H. & Dai, J. [1997] "Dynamical behavior, transient chaos, and riddled basins of two charged particles in a Paul trap," *Phys. Rev. A* **55**, 2159–2164.

Souza, S. L. T., Caldas, I. L. & Viana, R. L. [2007] "Damping control law for a chaotic impact oscillator," *Chaos Solit. Fract.* **32**, 745–750.

Sprott, J. C. [2003] *Chaos and Time-Series Analysis* (Oxford University Press, Oxford).

Srinivasan, K. [2008] "Doubling bifurcation route to chaos in periodically pulsed Murali–Lakshmanan–Chua (MLC) circuit," *Int. J. Bifurcation and Chaos* **18**, 541–555.

Tang, K. S., Man, K. F., Zhong, G. Q. & Chen, G. R. [2001] "Generating chaos via x mid x mid," *IEEE Trans. CAS I* **48**, 636–641.

Thompson, J. M. T. [1997] *Nonlinear Mathematics and Its Applications*, ed. Aston, P. J. (Cambridge University Press, Cambridge).

Ueda, Y. [1979] "Randomly transitional phenomena in the system governed by Duffing's equation," *J. Stat. Phys.* **20**, 181–196.

Ueda, Y. [1992] *The Road to Chaos* (Aerial Press, Santa Cruz).

van der Pol, B. [1926] "On relaxation-oscillations," *The London, Edinburgh, and Dublin Philos. Mag. J. Sci. Ser. 7* **2**, 978–992.

Wolf, A., Swift, J., Swinney, H. & Vastano, J. [1985] "Determining Lyapunov exponents from a time series," *Physica D* **16**, 285–317.

Yorke, J. A. & Yorke, E. D. [1979] "Metastable chaos: The transition to sustained chaotic oscillations in a model of Lorenz," *J. Stat. Phys.* **21**, 263–277.

Zhu, L., Raghu, A. & Lai, Y.-C. [2001] "Experimental observation of superpersistent chaotic transients," *Phys. Rev. Lett.* **86**, 4017–4020.